AIAA JOURNAL
Vol. 32, No. 9, September 1994

Laser Doppler Anemometry Data Simulation: Application to Investigate the Accuracy of Statistical Estimators

W. Fuchs* and H. Nobach†
University of Rostock, 18059 Rostock, Germany
and
C. Tropea‡
University of Erlangen-Nuremberg, 91058 Erlangen, Germany

Autoregressive models of order 1 are used to generate three-dimensional flowfields with specified probability distributions, spectra, and shear stress tensor. These known flowfields are then used to simulate the particle arrival statistics in laser Doppler anemometry for homogeneous particle densities. Further simulation steps allow modeling of the processor sampling and data acquisition, providing all necessary data for investigating the bias and variance of statistical estimators. Results are presented for estimators of the first two moments of the velocity distribution function. Experimental data are obtained for verification purposes. The results demonstrate the technique's potential for studying novel or theoretically intractable estimators.

Nomenclature

$A_{\perp v_k}$ = projected control volume area normal to instantaneous velocity vector
a, b, c = semiaxis lengths of ellipsoidal control volume
a_r, a_s, a_t = random noise sequences
b_r, b_s, b_t = random numbers: expectation zero, unity variance
C = symmetric coupling matrix, c_{ij}
h_n = random number sequence between 0 and 1
K = discretization factor of primary sequence
N_D = particle density (number particles/integral time scale ϑ_{ij})
N_ϑ = number of integral time scales
p = parameter describing normal stresses or Reynolds stresses
S_{ij} = power spectral density
T_s = data transfer period of one data point (Ref. 8)
V = volume of fluid passing control volume
v = discrete primary velocity series, (v_x, v_y, v_z)
z = discrete time AR sequences, (z_r, z_s, z_t)
β_1 = normalized statistical bias of velocity mean estimator
β_2 = normalized statistical bias of velocity variance estimator
Γ_v = Reynolds shear stress tensor, γ_{ij}
Δt = time step of primary sequence
$\overline{\Delta V}$ = mean volume of fluid passing control volume between particles
ϑ_{ij} = integral time scale matrix
ρ_{ij} = auto(cross)-correlation coefficients
τ = correlation lag time step
τ_n = residence time for nth particle
ϕ_r, ϕ_s, ϕ_t = autoregressive coefficients
$\langle\ \rangle$ = denotes estimate
$\overline{\ }$ = denotes time average

Received April 23, 1993; revision received Jan. 4, 1994; accepted for publication Jan. 7, 1994.

*Research Associate, Fachbereich Elektrotechnik, Einsteinstraße 2.
†Undergraduate Student, Fachbereich Elektrotechnik, Einsteinstraße 2.
‡Professor, Lehrstuhl für Strömungsmechanik, Cauerstraße 4.

Introduction

IT is well known that the particle arrival statistics in laser Doppler anemometry (LDA) may lead to large bias errors in estimators of time-averaged velocity moments, turbulence spectra, or, in fact, any particle-derived quantity. The origin of this potential statistical bias lies in the correlation between the measured velocity component and the velocity sampling function, i.e., particle arrivals in the measurement volume. How closely the velocity sampling function and the instantaneous particle rate are linked may further depend on a number of processor and data acquisition parameters, and thus these equipment parameters become an integral part of any given estimator.

For most commonly required flow quantities and for most available processing electronics, estimators have been proposed, and their performance in various flowfields has been the topic of a very large body of literature over the past years, both of an empirical and theoretical nature.[1] In fact, for many LDA applications the problem of choosing the most accurate estimator can be considered as being solved.

There remains, however, a substantial number of situations for which the prospects of a theoretical or experimental treatment are poor, or at least for which general disagreement about the correct approach still remains.[2] Examples of such situations include nonhomogeneously seeded flowfields, two-point LDA measurements, or the estimation of turbulence spectra in transient flowfields.

To study such cases in more detail, a numerical simulation approach has been developed. A simulation has the advantage over experimental studies that the correct answer is always known, and thus the absolute bias error and variance of each estimator can be evaluated. Furthermore, a computer simulation is usually more convenient than performing a series of systematic experiments in which many parameters must be very strictly controlled. Of course, this assumes that the simulation correctly models the desired process, and thus rigorous testing of the approach with known solutions or available data is mandatory before applying the technique to more novel situations.

The present paper describes a numerical simulation based on the generation of three-dimensional flowfields using autoregressive sequences. This simulation model is described in detail, after which verification results using well-known statistical estimators are presented. Experimental data have been obtained at high levels of turbulence as one example to illustrate the use of the simulation model to analyze practical

experimental situations and to evaluate estimator accuracy. Finally, the simulation model is used to investigate several LDA measurement situations that as yet have not been conclusively addressed in previous literature.

Both the simulation model and the experimental investigations are restricted to the case of single realization LDA; i.e., the probability of having more than one particle in the measuring volume at once is negligible. Furthermore, other sources of estimator bias or variance, such as the uncertainty of frequency estimation of individual Doppler signals, have not been addressed but are commented on in the conclusions.

Simulation Model

The simulation of LDA data from a three-dimensional turbulent flowfield with known statistical properties follows the approach taken in previous work[3] and is performed in a number of independent steps as represented diagrammatically in Fig. 1. Initially, a velocity time series, or *primary time series,* is generated at equidistant time points, which are closely spaced relative to flow time scales. This is performed using a first-order, trivariate autoregressive process with a Gaussian amplitude distribution. Second, the next particle distance from the control volume is generated according to the desired particle concentration model. In a conveyor-belt manner, the primary velocity series is integrated until the particle arrives in the control volume, yielding the arrival time. This is repeated for the next particle and so on, resulting in a *secondary time series* of particle velocities and arrival times. Since the velocity vector at the instant of particle arrival is known, a residence time can also be generated, knowing the measuring control volume (MCV) dimensions and assuming a random entrance position of the particle into the MCV. These two generation steps, i.e., primary and secondary time series, are described in detail later. A final simulation step allows consideration of the processor operating mode and the specifications of the hardware involved in the data acquisition and storage.

Primary Time Series

In the following discussion, the generation of a three-component velocity time series using a first-order autoregressive (AR) model is described. A higher order AR model offers no improvement in the modeling of the turbulence spectrum, and furthermore higher order models can no longer be expressed in closed form for programming.

A first-order AR process is used to generate three time sequences:

$$z_k = \begin{bmatrix} z_{r_k} \\ z_{s_k} \\ z_{t_k} \end{bmatrix} = \begin{bmatrix} \phi_r z_{r_{k-1}} + a_{r_k} \\ \phi_s z_{s_{k-1}} + a_{s_k} \\ \phi_t z_{t_{k-1}} + a_{t_k} \end{bmatrix} \tag{1}$$

with

$$a_{i_k} = \sqrt{1 - \phi_i^2}\, b_{i_k} \tag{2}$$

where the b_{i_k} values are normally distributed random numbers with expectation zero and unity variance. More detail concerning the properties and use of autoregressive functions can be found in Ref. 4. The desired simulated velocity vector is given by

$$v_k = Cz_k + \bar{v} = \begin{bmatrix} c_{xr} & c_{xs} & c_{xt} \\ c_{yr} & c_{ys} & c_{yt} \\ c_{zr} & c_{zs} & c_{zt} \end{bmatrix} \cdot \begin{bmatrix} z_{rk} \\ z_{sk} \\ z_{tk} \end{bmatrix} + \begin{bmatrix} \bar{v}_x \\ \bar{v}_y \\ \bar{v}_z \end{bmatrix} \tag{3}$$

Thus, the three time sequences $z_{r,s,t}$ are mapped by the coupling matrix C into three velocity components v_x, v_y, and v_z. Correlations between the fluctuations in each velocity component are contained in the symmetric coupling matrix C, which of course must be obtained from the Reynolds stress tensor Γ_v of the velocity field:

$$\Gamma_v = \begin{bmatrix} \gamma_{xx}, \gamma_{xy}, \gamma_{xz} \\ \gamma_{yx}, \gamma_{yy}, \gamma_{yz} \\ \gamma_{zx}, \gamma_{zy}, \gamma_{zz} \end{bmatrix} \tag{4}$$

The coefficients of the coupling matrix C can be obtained by iteratively solving the following set of equations:

$$\begin{aligned} \gamma_{xx} &= c_{xr}^2 + c_{xs}^2 + c_{xt}^2 \\ \gamma_{yy} &= c_{yr}^2 + c_{ys}^2 + c_{yt}^2 \\ \gamma_{zz} &= c_{zr}^2 + c_{zs}^2 + c_{zt}^2 \\ \gamma_{xy} = \gamma_{yx} &= c_{xr}c_{yr} + c_{xs}c_{ys} + c_{xt}c_{yt} \\ \gamma_{xz} = \gamma_{zx} &= c_{xr}c_{zr} + c_{xs}c_{zs} + c_{xt}c_{zt} \\ \gamma_{yz} = \gamma_{zy} &= c_{yr}c_{zr} + c_{ys}c_{zs} + c_{yt}c_{zt} \end{aligned} \tag{5}$$

The AR coefficients $\phi_{r,s,t}$ are obtained knowing the coefficients of the matrix C and prescribing the integral time scales of the three normal stresses, ϑ_{xx}, ϑ_{yy}, and ϑ_{zz}. The following equations can then be solved for $\phi_{r,s,t}$:

$$\vartheta_{xx} = \frac{1}{1-\phi_r} c_{xr}^2 + \frac{1}{1-\phi_s} c_{xs}^2 + \frac{1}{1-\phi_t} c_{xt}^2 \tag{6a}$$

$$\vartheta_{yy} = \frac{1}{1-\phi_r} c_{yr}^2 + \frac{1}{1-\phi_s} c_{ys}^2 + \frac{1}{1-\phi_t} c_{yt}^2 \tag{6b}$$

$$\vartheta_{zz} = \frac{1}{1-\phi_r} c_{zr}^2 + \frac{1}{1-\phi_s} c_{zs}^2 + \frac{1}{1-\phi_t} c_{zt}^2 \tag{6c}$$

The integral time scales of the Reynolds stress components are computed using

$$\vartheta_{xy} = \vartheta_{yx} = \frac{1}{1-\phi_r} c_{xr}c_{yr} + \frac{1}{1-\phi_s} c_{xs}c_{ys} + \frac{1}{1-\phi_t} c_{xt}c_{yt} \tag{7a}$$

$$\vartheta_{xz} = \vartheta_{zx} = \frac{1}{1-\phi_r} c_{xr}c_{zr} + \frac{1}{1-\phi_s} c_{xs}c_{zs} + \frac{1}{1-\phi_t} c_{xt}c_{zt} \tag{7b}$$

$$\vartheta_{yz} = \vartheta_{zy} = \frac{1}{1-\phi_r} c_{yr}c_{zr} + \frac{1}{1-\phi_s} c_{ys}c_{zs} + \frac{1}{1-\phi_t} c_{yt}c_{zt} \tag{7c}$$

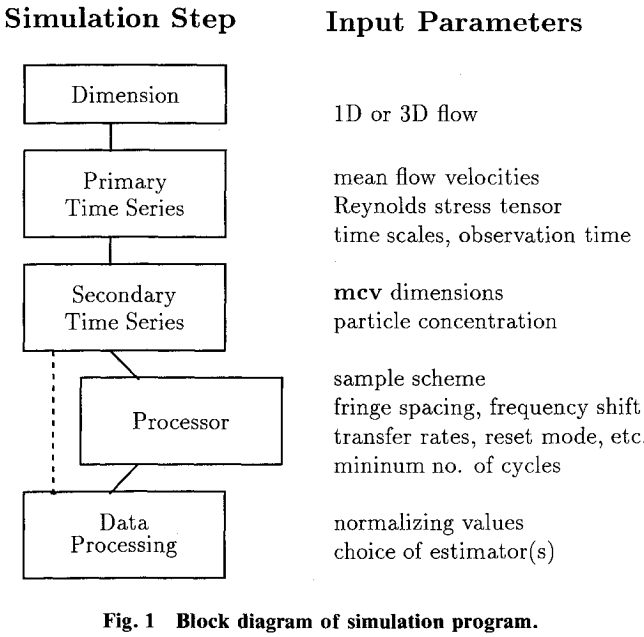

Fig. 1 Block diagram of simulation program.

The time step of the z_k sequences is chosen such that there are K steps in one integral time scale in the x direction (v_x component), i.e.,

$$\Delta t = \frac{\vartheta_{xx}}{K} \tag{8}$$

To summarize, the mean velocity vector; the Reynolds stress tensor [Eq. (4)]; and ϑ_{xx}, ϑ_{yy}, and ϑ_{zz} are prescribed. The coupling matrix C is obtained by solving Eq. (5) iteratively. Equations (6a–6c) are then used to obtain $1/(1-\phi_i)$, which are then substituted into Eqs. (7a–7c) to yield ϑ_{xy}, ϑ_{xz}, and ϑ_{yz}. The AR coefficients ϕ_i are used in Eqs. (1–3) to obtain the velocity vector time series.

It is assumed that the LDA measurement is made with respect to the x direction. The probability density function is determined by the distribution used for the b_i random numbers, in this case a Gaussian distribution. The variances are given by the diagonal coefficients of the Reynolds shear stress tensor. The power spectral density of, for instance, the x component of velocity may be expressed as

$$S_{xx}(f) = \frac{2c_{xr}^2(1-\phi_r^2)}{1+\phi_r^2-2\phi_r\cos 2\pi f} + \frac{2c_{xs}^2(1-\phi_s^2)}{1+\phi_s^2-2\phi_s\cos 2\pi f} + \frac{2c_{xt}^2(1-\phi_t^2)}{1+\phi_t^2-2\phi_t\cos 2\pi f} \tag{9}$$

where f is normalized with the time step, taking values between 0 and 0.5. The autocorrelation and cross-correlation coefficients are given by

$$\begin{aligned}
\rho_{xx}(\tau) &= (\phi_r^\tau c_{xr}^2 + \phi_s^\tau c_{xs}^2 + \phi_t^\tau c_{xt}^2)/\gamma_{xx} \\
\rho_{yy}(\tau) &= (\phi_r^\tau c_{yr}^2 + \phi_s^\tau c_{ys}^2 + \phi_t^\tau c_{yt}^2)/\gamma_{yy} \\
\rho_{zz}(\tau) &= (\phi_r^\tau c_{zr}^2 + \phi_s^\tau c_{zs}^2 + \phi_t^\tau c_{zt}^2)/\gamma_{zz} \\
\rho_{xy}(\tau) = \rho_{yx}(\tau) &= (\phi_r^\tau c_{xr}c_{yr} + \phi_s^\tau c_{xs}c_{ys} + \phi_t^\tau c_{xt}c_{yt})/\gamma_{xy} \\
\rho_{xz}(\tau) = \rho_{zx}(\tau) &= (\phi_r^\tau c_{xr}c_{zr} + \phi_s^\tau c_{xs}c_{zs} + \phi_t^\tau c_{xt}c_{zt})/\gamma_{xz} \\
\rho_{zy}(\tau) = \rho_{yz}(\tau) &= (\phi_r^\tau c_{zr}c_{yr} + \phi_s^\tau c_{zs}c_{ys} + \phi_t^\tau c_{zt}c_{yt})/\gamma_{zy}
\end{aligned} \tag{10}$$

Secondary Time Series

The primary time series is used to generate a secondary data set consisting of particle velocities (x component), arrival times, and residence times, similar to the data available from an LDA signal processor. To achieve this, the particle density and the measurement volume dimensions must be prescribed. The particle density N_D is prescribed as the number of particle arrivals per integral time scale of the x-velocity component. The ellipsoidal measurement volume is prescribed by the lengths of the three semiaxes a, b, and c for the directions x, y, and z, respectively. Thus particle detection is an on-off function described by the ellipsoid and will not take into account the dependence of detection probability on particle size.

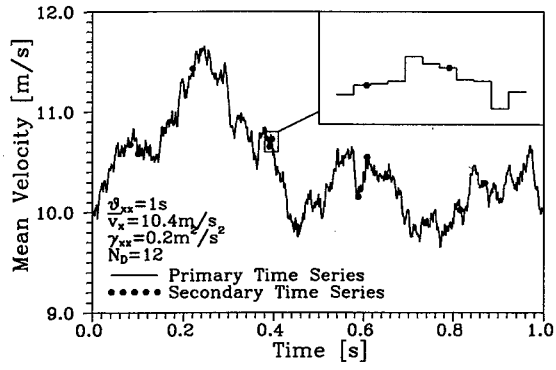

Fig. 2 Graphic representation of example primary and secondary (particle) time series.

Table 1 Summary of simulation conditions for results in Fig. 3

Mean velocity, m/s	7.698
Variance, m²/s²	4.01
Integral time scale, ms	2.3
MCV diameter, μm	160
Shift frequency, MHz	5
Fringe spacing, μm	3.785
Minimum periods	8
Particle density	Variable

According to the conveyor-belt model, the distance to the next particle along the fluid filament passing through the control volume must be generated, after which the primary time series is integrated until the particle arrives in the volume, yielding the arrival time. For a homogeneously seeded flow the distance between particles is exponentially distributed. In contrast to a one-dimensional conveyor-belt model, however, the present model must also take into account that directional changes of the velocity vector will result in a change of the projected control volume area, thus affecting the number of particles "seen" by the system. Therefore this model uses exponentially distributed *volumes* of fluid filaments between adjacent particles. The task lies alone in determining which mean volume between particles ($\overline{\Delta V}$) is to be used.

This mean value is obtained by first expressing the total volume of fluid passing through the control volume over a period of N_ϑ integral time scales as

$$V = \overline{\Delta V} \cdot N_D \cdot N_\vartheta \tag{11}$$

This volume of fluid can, however, also be obtained by integrating the product of the instantaneous velocity vector and the projected control volume area normal to this vector, approximated by[5]

$$V = \Delta t \sum_{k=1}^{KN_\vartheta} A_{\perp v_k} |v_k| \tag{12}$$

The quantity V is computed once for each time series. For each required mean particle density the mean volume between particles $\overline{\Delta V}$ can then be computed by equating Eqs. (11) and (12):

$$\overline{\Delta V} = \frac{\Delta t \sum_{k=1}^{KN_\vartheta} |v_k| A_{\perp v_k}}{N_D N_\vartheta} = \frac{\pi abc}{N_D N_\vartheta} \Delta t \sum_{k=1}^{KN_\vartheta} \left(\frac{v_{xk}^2}{a^2} + \frac{v_{yk}^2}{b^2} + \frac{v_{zk}^2}{c^2}\right)^{1/2} \tag{13}$$

The actual volumes between particles is generated in a random manner according to

$$\Delta V_n = -\ell n(1-h_n) \cdot \overline{\Delta V} \tag{14}$$

where h_n is a random number with uniform probability between 0 and 1.

Note that in Eq. (12) a summation is used to approximate the integrated vector velocity. The accuracy of this approximation increases with decreasing Δt (or increasing K). For $K \geq 100$, no appreciable improvement in this approximation is obtained. The arrival time of the next particle t_n is therefore given implicitly by the integral equation

$$\Delta V_n = \int_{t_{n-1}}^{t_n} A_{\perp v_k} \cdot |v_k| \, dt \tag{15}$$

This equation is solved for t_n, again using a summation to approximate the integral.

The residence time for each particle τ_n is generated by assuming random entrance points into the measurement volume, equally distributed over the projected volume normal to

Table 2 Summary of estimators for mean and variance of velocity

Estimator	Designation	Processor mode	Weight α_i	Expected mean bias
Ensemble	E	Free running	1	Ref. 9
Arrival time	AT	Free running	Δt_i	—
Transit time	TT	Free running	τ_i	Ref. 10
Controlled	CP	Control epochs, T_s	1	Ref. 8
Sample and hold	SH	Equidistant, T_s	1	Refs. 11 and 12

Arrival time $\Delta t_i = t_i - t_{i-1}$

Residence time τ_i

Mean estimator $\langle v_x \rangle = \frac{\Sigma_1^N v_{xi}\alpha_i}{\Sigma_1^N \alpha_i}$

Variance estimator $\langle \gamma_{xx} \rangle = \frac{\Sigma_1^N (v_{xi} - \langle v_x \rangle)^2 \alpha_i}{\Sigma_1^N \alpha_i}$

the instantaneous velocity vector. The secondary time series consists therefore of a data set with three values per event: x-velocity component v_{xn}, arrival time t_n, and residence time τ_n. In Fig. 2 a typical primary time series over a period of one integral time scale is shown with the particle arrivals for a particle density of 12 particles per integral time scale.

Processor Series

If it can be assumed that all particles are processed and only one frequency value per particle is used, the data processing can be performed directly on the secondary time series (particle series) without including any further simulation steps. In general, however, it is desirable to include a final simulation step in which the influence of the LDA processor and the computer interface are considered. In this step it is assumed that all particles follow the flow exactly, that the probability of two or more particles in the measuring volume at any one time is negligible, and that the velocity (frequency) can be determined with infinite accuracy, i.e., the variance of the frequency estimator is zero. Provision is made for specifying maximum data transfer rates, dead times, reset times, and possible buffer overflows. A minimum and a maximum number of periods required for frequency estimation or alternatively an end-of-burst criterion can also be specified.

The particle arrival time given in the secondary time series is considered to be the time at which the particle is in the middle of the measurement control volume. The first signal detection instant is therefore this arrival time minus half the residence time.

The processing mode must be specified at this simulation step. Three possibilities are provided: the free-running processor, in which every particle is acquired; the controlled processor, in which all but the first particle arriving after periodic enable epochs are discarded; and the resampling processor ($S + H$), in which data are read at equidistant sample times, using the last valid particle value. Together with the specified hardware parameters, most common LDA systems can be modeled. For instance, a processor that performs multiple measurements per burst can be simulated since the Doppler frequency, the residence time, and the frequency shift are all known quantities in the program. For this case a free-running processor with very short reset times and no end-of-burst detection can be used.

The output from the processor simulation step is now a set of data consisting of three values per event: an x-velocity component, an arrival time, and a residence time. The arrival time corresponds to the time at which the processor completed its signal validation or the time at which the velocity value was received at the interface, depending on the exact hardware configuration specified. Note that the number of events in the *processor series* may differ substantially, either more or less, than the number of events in the secondary time series. Utility programs can be used at this stage to convert the data sets into a format resembling experimental data, allowing further processing using available laboratory software.

Figure 1 indicates the various steps in the computer simulation. The data generated at each step can also be stored in files. Thus systematic parameter variations and their effect on a common simulated time series can easily be investigated. Note that this simulation model resembles previous models used for the same purpose[6,7]; however, it extends the capabilities to include hardware-related parameters and refines the flow model, especially with respect to the third velocity component.

Verification of Simulation Model

To verify the simulation model, the dependency of several mean estimators on the data density has been investigated and compared either with known theoretical dependencies or with experimental data obtained under carefully controlled conditions. The experimental work is taken from Ref. 8, for which all essential information is available, e.g., integral time scale, interface dead times, turbulence intensity (26%), etc. A primary time series was first generated, matching the known experimental conditions. Using this primary series, several particle series were then generated ranging in data densities between 0.1 and 30. Note that a one-dimensional simulation was used, after first confirming that no significant differences to a three-dimensional simulation were apparent for turbulence levels under 30%.[7] The data used for this simulation are summarized in Table 1.

The mean and variance estimators investigated are summarized in Table 2, with appropriate reference to available theoretical solutions that describe their dependency on data density. In the following presentation of results, the normalized statistical biases β_1 and β_2 (in percent) are used to evaluate the mean and variance estimators, respectively,

$$\beta_1 = \frac{\langle v_x \rangle - \bar{v}_x}{\bar{v}_x} \tag{16}$$

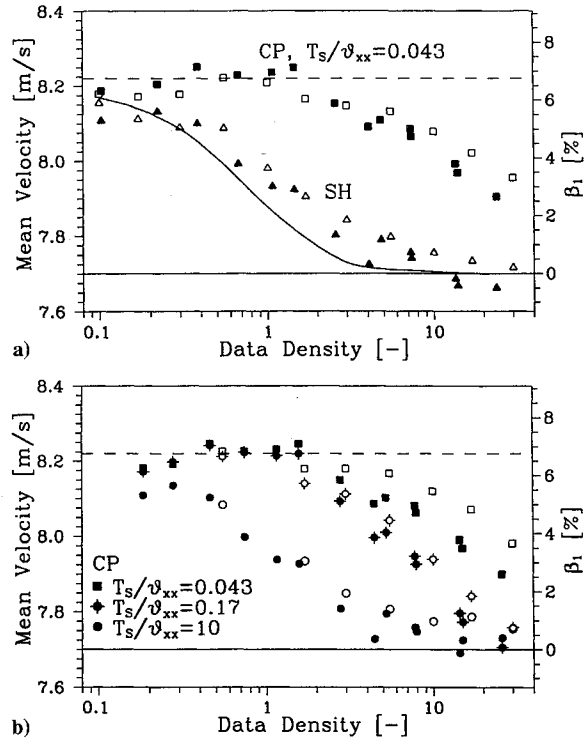

Fig. 3 Comparison of simulation results to theory and experiments[8]: - - -, $\beta_1 = \gamma_{xx}/\overline{v_x}^2$; ——, $S + H$ model[8]; open symbols, simulations; and solid symbols, experiments: a) $S + H$ and controlled processor at 26% turbulence level and b) controlled processor for various control intervals.

Table 3 Summary of final simulation parameters and LDA system parameters for data presented in Fig. 4

	x	y	z
Mean velocity, m/s	0.432	0.180	0.134
Variance, m^2/s^2	0.189	0.158	0.170
Covariance to x, m^2/s^2	—	−0.032	−0.062
Integral time scale, ms	11	1.5	1.5
MCV diameter, μm	19	19	140
Shift frequency, kHz	500		
Fringe spacing, μm	3.17		
Minimum periods	8		
Particle density	Variable		

$$\beta_2 = \frac{\langle \gamma_{xx} \rangle - \gamma_{xx}}{\gamma_{xx}} \tag{17}$$

In Fig. 3a the results for a controlled processor and a sample and hold processor are compared. The controlled processor was in fact unintentional but arose because of a 10.4-kHz maximum data transfer rate in the experiments ($T_s/\vartheta_{xx} = 0.043$).[8] Agreement between experiment, theory, and simulations is excellent, confirming that the simulation model captures the essential features of the system. The deviation between the theoretical and experimental/simulated data for the sample and hold processor indicates that the $S + H$ model proposed by Winter et al.[8] may be at fault, rather than the measured integral time scale, since the simulations were performed with the measured value of $\vartheta_{xx} = 2.3$ ms, resulting in good agreement with the experiments.

In Fig. 3b further comparisons between different controlled processors also show excellent agreement. The upper limit of mean velocity bias, $\beta_1 = \gamma_{xx}/\overline{v_x}^2$ (free-running processor), is achieved for both the controlled processor and the sample and hold processor at low data densities, as expected.

Comparison with Experiments

In the following comparison, the simulation model is used to "post"-dict LDA measurements taken in a flow with a high turbulence level. The procedure used for postdiction and the behavior of several mean and variance estimators at high turbulence levels are illustrated.

The flow chosen for investigation was that over a surface-mounted cube placed in a fully developed channel flow, for which a detailed study using LDA has been performed by Martinuzzi.[13] A measurement position in the wake of the obstacle was chosen at which the turbulence level was approximately 100%. Measurements were performed using a single-component, backscatter LDA system and a counterprocessor interfaced to a PC computer. Table 3 summarizes the system parameters.

Measurements of the streamwise (x) and cross-stream (z) velocity components were performed, yielding estimates of $\overline{v_x}$, $\overline{v_z}$, γ_{xx}, γ_{zz}, ϑ_{xx}, and ϑ_{zz}. These measurements were repeated for four values of data density between 0.2 and 6.4. Data from Ref. 13 were used to estimate $\overline{v_y}$ and γ_{yy} and for the Reynolds shear stresses. The time scale ϑ_{yy} was set equal to ϑ_{zz}.

The problem of flow simulation now becomes evident. All of the aforementioned values are only estimates, for which the actual bias is unknown. Therefore the simulation must be performed iteratively. An initial primary series is generated using the previous estimates (transit time weighted estimates were used), from which secondary time series at different data densities can be obtained. The simulation results for three mean estimators—ensemble (E), arrival time (AT), and transit time (TT)—are then compared with the corresponding experimental results. This procedure is repeated, making small adjustments to the simulation input flow parameters, until good agreement is achieved with the experimental results. The final set of flow simulation parameters represents the true flow parameters.

The final comparison between simulation and experiment is illustrated in Fig. 4 for the mean velocity and the velocity variance. The final set of input flow parameters is given in Table 3. The ensemble bias parameter β_1, although independent of data density, is now much lower than $(\gamma_{xx}/\overline{v_x}^2)$, i.e., the case for a one-dimensional turbulence field. The arrival time estimator becomes reliable only at data densities exceeding 20.

The variance bias parameter β_2, shown in Fig. 4b, is independent of data density for all estimators investigated. Although the transit time estimator provides accurate mean velocities, the variance shows a bias of up to −20%. The arrival time estimator appears to provide the most accurate variance at this turbulence level. Whether this conclusion is valid for all turbulence levels is a question that is easily investigated using the simulation model, as described in the next section.

Additional dashed curves are included in Fig. 4 to illustrate the importance of including the processor functions in the simulation. The dashed lines represent the simulation estimates derived directly from the particle series. The deviation between these estimates and the simulations, including the processor simulation step, arise due to the minimum cycle requirement that was used in the measurements (eight cycles). Clearly this constraint strongly affected which set of particles were evaluated, leading to the conclusion that the shift frequency was chosen too small in this experiment! This is one example therefore of how the simulation model can be used to retroactively analyze an LDA experiment.

Example Application

An important application of the simulation model is to analyze measurement situations for which theoretical estimates of bias errors are not available. One such situation is very high turbulence levels, such as are encountered in separated flow regions.

To study the influence of turbulence intensity on various estimators, simulations were carried out for the flowfield

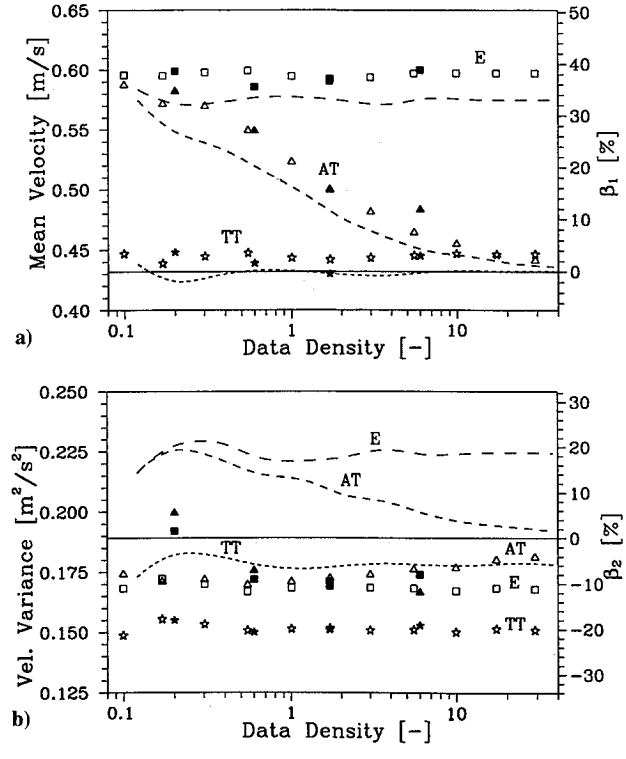

Fig. 4 Comparison of simulated results of a) mean velocity and b) velocity variance with experimental measurements: open symbols, simulation; solid symbols, experiment; and dashed lines, without processor simulation.

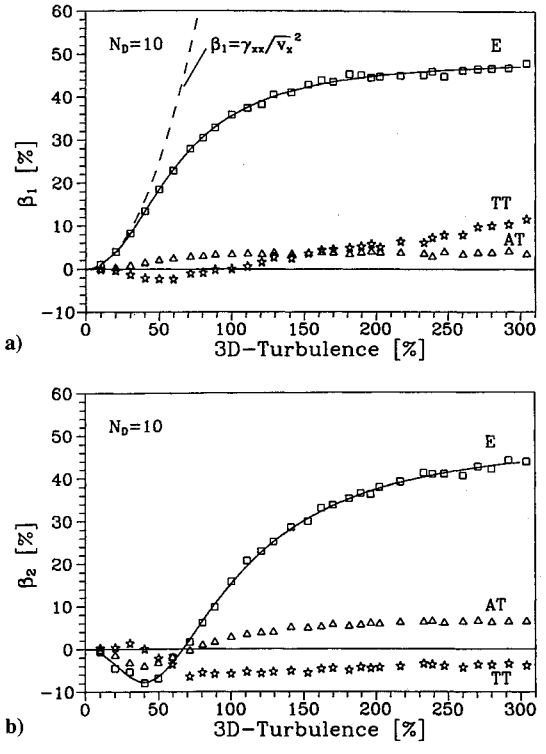

Fig. 5 Simulated a) mean velocity and b) velocity variance estimators as a function of turbulence intensity.

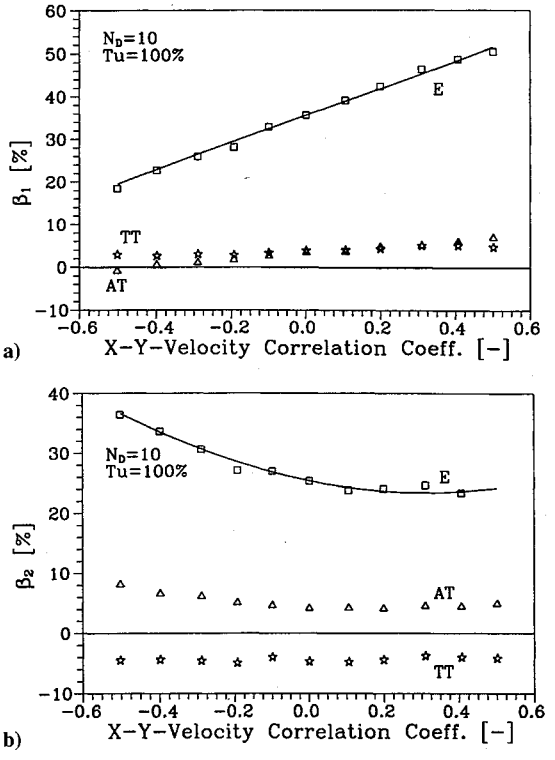

Fig. 6 Simulated a) mean velocity and b) velocity variance estimators as a function of Reynolds shear stress coefficient.

$$\bar{v} = \begin{bmatrix} 1 \\ 0 \\ 0 \end{bmatrix} \qquad \Gamma_v = \begin{bmatrix} p & 0 & 0 \\ 0 & p & 0 \\ 0 & 0 & p \end{bmatrix} \tag{18}$$

where the iteration parameter p was chosen to yield turbulence levels between 10 and 300%. Results of this study are summarized in Fig. 5 for the mean velocity and velocity variance, using a particle density of $N_D = 10$.

As expected, the ensemble estimator of the mean velocity follows the $\beta_1 = (\gamma_{xx}/\overline{v_x}^2)$ relation for low turbulence levels but levels off for higher values since both positive *and* negative velocities are biased towards higher absolute values. The variance is initially underestimated but then becomes too large above turbulence levels of approximately 70%.

The transit time mean estimator shows initially a negative bias but then increases steadily with increasing turbulence. Presumably there are several competing effects responsible for this behavior. Accurate estimates are obtained for turbulence levels near 100%. For very high turbulence levels the arrival time estimate appears to be most reliable, at least for this particle density.

The previous example is somewhat artificial in that the turbulence level has been increased without any contributions to the shear stresses. On the other hand, the shear stresses do not affect the mean estimates as long as the mean velocities $\overline{v_y}$ and $\overline{v_z}$ are zero, since the influence is symmetric about zero. The variance estimators can, however, be affected.

A further example taken at a turbulence level of 100% investigates the influence of the Reynolds shear stress. This example is of a measurement taken at 45 deg to the main flow direction, a typical alignment when a one-component LDA system is used to measure Reynolds shear stresses in a stationary flow. In this investigation the flowfield was given by

$$\bar{v} = \begin{bmatrix} 1/\sqrt{2} \\ 1/\sqrt{2} \\ 0 \end{bmatrix} \qquad \Gamma_v = \begin{bmatrix} 1 & p & 0 \\ p & 1 & 0 \\ 0 & 0 & 1 \end{bmatrix} \tag{19}$$

where p is again the iteration parameter. The results are presented in Fig. 6.

In this case the ensemble mean estimate shows a strong dependence on the Reynolds shear stress, since the Reynolds shear stress now directly influences how well correlated the volume flow rate through the MCV is with the measured velocity component. Expectedly, the variance also shows an asymmetric behavior. Clearly both the arrival time estimator and the transit time estimator are superior in this situation.

Concluding Remarks

The purpose of this paper was to introduce a flexible simulation model for the investigation of LDA flow estimators and to document its reliability through the presentation of several comparisons and examples. In the meantime, the model has been successfully used in a wide variety of studies, of which a few can be mentioned as examples:

1) By modulating the mean filament volume $\overline{\Delta V}$ with the instantaneous flow velocity, the model can be extended to account for nonhomogeneously seeded flows.[7]

2) After generating a three-dimensional primary series with known cross correlations (Reynolds shear stresses), the three velocity components have been separated and three individual particle series have been obtained. These series are used to evaluate cross-correlation estimators, as are required when acquiring data from a two-point LDA system.[14]

3) The simulation model has been used to evaluate various schemes of signal reconstruction, with the aim of performing a spectral analysis on the equidistantly resampled data set.

This illustrates the flexibility and potential of the technique for studying future applications of the laser Doppler anemometer.

At the same time the limitations of this simulation model must be stressed. Essentially only the bias and uncertainty related to particle statistics are isolated and addressed. In any given experimental situation, however, many other sources of bias may become predominant. In particular, the variance of the frequency estimate increases with decreasing signal-to-noise ratio (e.g., photon noise or optical propagation effects), lead-

ing to a bias of the velocity moment estimators and to distortions of spectral estimators. Another important source of error not considered is the variance of the transit time, which is also sensitive to the signal quality. Experience shows that at low signal-to-noise ratios this is the main limiting factor to employing transit time weighting, especially since estimation errors are weighted towards larger values and can be substantial. It is therefore important to recognize that the present work must be considered in conjunction with other possible uncertainties. For successful comparisons and verifications of simulations generated by this program with experimental data, it is therefore necessary to insure high signal quality in the experiments to minimize such distorting influences.

Acknowledgments

This work has been financially supported by the Volkswagen Foundation under Contract I/66 487. The simulation model described in this work is available as an executable program for PC computers. The authors are pleased to make this program and an accompanying handbook available to any interested readers.

References

[1]*Proceedings of 1st-6th International Symposium on Applications of Laser Anemometry to Fluid Mechanics,* LADOAN, Lisbon, Portugal, 1982, 1984, 1986, 1988, 1990, 1992.

[2]Edwards, R. V. (ed.), "Report of the Special Panel on Statistical Particle Bias Problems in Laser Anemometry," *Transactions of the ASME, Journal of Fluids Engineering,* Vol. 109, June 1987, pp. 89–93.

[3]Tropea, C., "Turbulence-Induced Spectral Bias in Laser Anemometry," *AIAA Journal,* Vol. 25, No. 2, 1987, pp. 306–309.

[4]Box, G. P., and Jenkins, G. M., *Time Series Analysis—Forecasting and Control,* Holden-Day, Oakland, CA, 1976.

[5]Buchhave, P., "Biasing Errors in Individual Particle Measurements with the LDA Counter Signal Processor," *Proceedings of the LDA-Symposium Copenhagen,* Proceedings LDA-Symposium Copenhagen 1975, P.O. Box 70, Skovlunde, Denmark, 1976, pp. 258–278.

[6]Buchhave, P., von Benzon, H.-H., and Rasmussen, C. N., "LDA Bias: Comparison of Measurement Errors from Simulated and Measured Data," *Proceedings of the 5th International Symposium on Applications of Laser Techniques to Fluid Mechanics,* Paper 29.3, LADOAN, Lisbon, Portugal, 1990.

[7]Fuchs, W., Albrecht, H., Nobach, H., Tropea, C., and Graham, L., "Simulation and Experimental Verification of Statistical Bias in Laser Doppler Anemometry Including Non-Homogeneous Particle Density," *Proceedings of the 6th International Symposium on Applications of Laser Techniques to Fluid Mechanics,* Paper 8.2, LADOAN, Lisbon, Portugal, 1992.

[8]Winter, A. R., Graham, L. J. W., and Bremhorst, K., "Velocity Bias Associated with Laser Doppler Anemometer Controlled Processors," *Transactions of the ASME, Journal of Fluids Engineering,* Vol. 113, June 1991, pp. 250–255.

[9]Erdmann, J. C., and Tropea, C., "Statistical Bias of the Velocity Distribution Function in Laser Anemometry," *Proceedings of the International Symposium on Applications of LDA to Fluid Mechanics,* Paper 16.2, LADOAN, Lisbon, Portugal, July 1982.

[10]Buchhave, P., George, W. K., Jr., and Lumley, J., "The Measurement of Turbulence with the Laser Doppler Anemometer," *Annual Review of Fluid Mechanics,* Vol. 11, Annual Reviews, Inc., Palo Alto, CA, 1979, pp. 442–503.

[11]Edwards, R. V., and Jensen, A. S., "Particle-Sampling Statistics in Laser Anemometers: Sample-and-Hold Systems and Saturable System," *Journal of Fluid Mechanics,* Vol. 133, 1983, pp. 397–411.

[12]Winter, A. R., Graham, L. J. W., and Bremhorst, K., "Effects of Time Scales on Velocity Bias in LDA Measurements Using Sample and Hold Processing," *Experiments in Fluids,* Vol. 11, 1991, pp. 147–152.

[13]Martinuzzi, R., "Experimentelle Untersuchung der Umströmung wandgebundener, rechteckiger, prismatischer Hindernisse," Dissertation, Lehrstuhl für Strömungsmechanik, Univ. of Erlangen-Nürnberg, Erlangen, Germany, 1992.

[14]Benak, M., Sturm, M., Tropea, C., Nobach, H., Fuchs, W., and Müller, E., "Correlation Estimators for Two-Point Laser Doppler Anemometry," *Laser Anemometry: Advances and Applications—Proceedings of the 5th International Conference,* edited by J. M. Bessem, R. Booij, H. Godefroy, P. J. de Groot, K. Krishna Prasad, F. F. M. de Mul, and E. J. Nijhof, Society of Photo-Optical Instrumentation Engineers, Bellingham, WA, Proc. SPIE 2052, 1993, pp. 613–622.